Trapped Tyrosyl Radical Populations in Modified Reaction Centers from *Rhodobacter sphaeroides*†

A. J. Narváez,‡ R. LoBrutto,§ J. P. Allen,*,‡ and J. C. Williams‡

Department of Chemistry and Biochemistry and School of Life Sciences, Arizona State University, Tempe, Arizona 85287

Received June 23, 2004; Revised Manuscript Received August 28, 2004

ABSTRACT: The photosynthetic reaction center from the purple bacterium *Rhodobacter sphaeroides* has been modified such that the bacteriochlorophyll dimer, when it becomes oxidized after light excitation, is capable of oxidizing tyrosine residues. One factor in this ability is a high oxidation−reduction midpoint potential for the dimer, although the location and protein environment of the tyrosine residue appear to be critical as well. These factors were tested in a series of mutants, each of which contains changes, at residues L131, M160, M197, and M210, that give rise to a bacteriochlorophyll dimer with a midpoint potential of at least 800 mV. The protein environment was altered near tyrosine residues that are either present in the wild type or introduced by mutagenesis, focusing on residues that could act as acceptors for the phenolic proton of the tyrosine upon oxidation. These mutations include Ser M190 to His, which is near Tyr L162, the combination of His M193 to Tyr and Arg M164 to His, which adds a Tyr−His pair, and the combinations of Arg L135 to Tyr with Tyr L164 to His, Arg L135 to Tyr with Tyr L144 to Glu, and Arg L135 to Tyr with Tyr L164 to Phe. Radicals were produced in the mutants by using light to initiate electron transfer. The radicals were trapped by freezing the samples, and the relative populations of the oxidized dimer and tyrosyl radicals were determined by analysis of low-temperature electron paramagnetic resonance spectra. The mutants all showed evidence of tyrosyl radical formation at high pH, and the extent of radical formation at Tyr L135 with pH differed depending on the identity of L144 and L164. The results show that tyrosine residues within approximately 10 Å of the dimer can become oxidized when provided with a suitable protein environment.

The photosynthetic reaction center from the purple bacterium *Rhodobacter sphaeroides* is an integral membrane−protein pigment complex responsible for conversion of electromagnetic energy into chemical energy (*1*). It contains three subunits called L, M, and H, with the L and M subunits forming the core that binds the cofactors with a 2-fold symmetry (*2*). After excitation by light, an electron is transferred from the bacteriochlorophyll dimer, P,[1] forming the oxidized state, P^+, to a bacteriopheophytin, H_A, and then to a primary and secondary quinone electron acceptor. The bacteriochlorophyll dimer possesses a midpoint potential of approximately 0.5 V, while, in contrast, the primary electron donor from photosystem II operates at a midpoint potential of approximately 1.1 V (*3*). The latter possesses the capability to oxidize specific tyrosine residues, which have midpoint potentials of approximately 0.7 and 1.0 V (*4*, *5*). In *R. sphaeroides*, protein interactions have been identified that affect the redox potential of the primary donor and, in particular, that increase the midpoint potential substantially (*6*−*8*). For example, by specific alteration in the hydrogen bond pattern of the bacteriochlorophyll dimer achieved through introducing histidine residues at positions L131, M160, and M197, the midpoint potential can be raised by approximately 0.26 V (*7*). Other studies have shown that replacement of Tyr M210 with Trp results in an increase in the midpoint potential of the dimer by approximately 0.06 V (*6*). Combination of these four changes that increase the redox potential in the so-called quadruple mutant provides the dimer with enough redox capability to oxidize tyrosine residues when they are introduced at M164 and L135 in the Y_{M164} and Y_{L135} mutants, previously referred to as the Y_M and Y_L mutants, respectively (*9*). The introduced tyrosines are located at positions corresponding to those of the redox-active tyrosines of photosystem II (*10*−*12*).

The redox-active tyrosine Y_Z in photosystem II has been shown to play a significant role in the water oxidation process through transfer of both electrons and protons (*13*−*17*). In these models, oxidation of Y_Z is coupled to proton transfer to yield a neutral tyrosyl radical. Reduction of this residue

† This work was supported by Grant MCB 0131764 from the NSF.

* To whom correspondence should be addressed. Phone 480-965-8241. Fax: 480-965-2747. E-mail: jallen@asu.edu.

‡ Department of Chemistry and Biochemistry, Arizona State University.

§ School of Life Sciences, Arizona State University.

[1] Abbreviations: EPR, electron paramagnetic resonance; H_A, bacteriopheophytin in the active branch of cofactors; P, bacteriochlorophyll dimer; quadruple, mutant with high P/P^+ midpoint potential; Y_{L135}, mutant with high P/P^+ midpoint potential and redox-active tyrosine at residue L135; Y_{L135} + YH(L164), mutant with high P/P^+ midpoint potential, redox-active tyrosine at residue L135, and Tyr to His mutation at residue L164; Y_{L135} + YH(L164) + YE(L144), mutant with high P/P^+ midpoint potential, redox-active tyrosine at residue L135, Tyr to His mutation at residue L164, and Tyr to Glu mutation at residue L144; Y_{L135} + YF(L164), mutant with high P/P^+ midpoint potential, redox-active tyrosine at residue L135, and Tyr to Phe mutation at residue L164; Y_{L162} + SH(M190), mutant with high P/P^+ midpoint potential, redox-active tyrosine at residue L162, and Ser to His mutation at residue M190; Y_{M164}, mutant with high P/P^+ midpoint potential and redox-active tyrosine at residue M164; Y_{M193} + RH(M164), mutant with high P/P^+ midpoint potential, redox-active tyrosine at residue M193, and Arg to His mutation at residue M164.

10.1021/bi048691p CCC: $27.50
Published on Web 10/23/2004

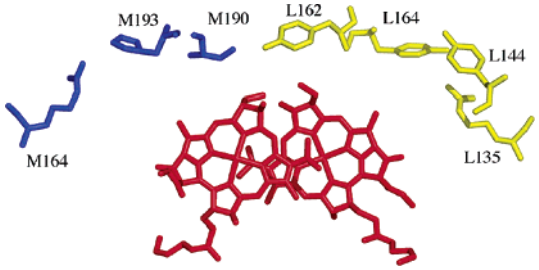

FIGURE 1: View of the bacteriochlorophyll dimer (red), nearby amino acid residues of the L subunit (yellow), Arg L135, Tyr L144, Tyr L162, and Tyr L164, and nearby amino acid residues of the M subunit (blue), Arg M164, Ser M190, and His M193, in wild-type reaction centers from *R. sphaeroides*. Arg L135 is located approximately 10 Å from the edge of the bacteriochlorophyll dimer, 3 Å from Tyr L164, and 5 Å from Tyr L144. Arg M164 is located approximately 10 Å away from the edge of the dimer and 3 Å from the M193 site. Tyr L162 is located approximately 6.5 Å away from the edge of the dimer and 4.3 Å away from Ser M190.

by the manganese cluster may be coupled to protonation via water molecules bound to the cluster. Formation of the tyrosyl radical occurs with the aid of a nearby histidine residue that acts as a proton acceptor to the phenolic proton (*18*, *19*). Generation of the tyrosyl radical is highly dependent on pH, most likely because of the protonation state of residues that act as proton acceptors of the phenolic proton upon formation of the radical. For example, in the reaction center, His M193 is likely the major proton acceptor for the redox-active tyrosine at M164 while Glu M173 apparently interacts weakly with the tyrosine (*20*). Radical formation at Tyr L135 occurs with a well-defined transition at pH 8.3, higher than the pK_a of 6.9 observed for radical formation at Tyr M164, showing the influence of the different protein environments (*9*, *21*). Two nearby residues, Tyr L164 and Tyr L144, may play a role in accepting the phenolic proton of Tyr L135 (Figure 1).

To test the effect of altering the protein environment on the oxidation of tyrosine residues by high-potential bacteriochlorophyll dimers in the reaction center from *R. sphaeroides*, five mutants were constructed and compared to the Y_{L135}, Y_{M164}, and quadruple mutants (Table 1). The Y_{L162} + SH(M190) mutant is designed to provide a proton acceptor to Tyr L162, located approximately 6.5 Å away from the edge of the dimer (Figure 1). This tyrosine is present in the wild type and in the quadruple mutant located near a glycine residue, two asparagine residues, and Ser M190. Insertion of a His at M190 may form a hydrogen bond to a Tyr L162 and so provide a pathway for proton transfer of the phenolic proton upon oxidation of the tyrosine. In the Y_{M193} + RH(M164) mutant, placing a tyrosine at position M193 and a histidine at position M164 creates another possible tyrosine−proton acceptor pair. In three mutants based on the Y_{L135} mutant, residues Tyr L164 and Tyr L144 were altered to change the environment near Tyr L135. In one of these mutants Tyr L164 was replaced with His, and a second mutant combined the replacement of Tyr L164 with His and the replacement of Tyr L144 with Glu. These mutants should make the environment more similar to that in the M-side tyrosine mutants since L164 and L144 are symmetry related to His M193 and Glu M173, respectively. In the third mutant, Tyr L164 was replaced with Phe, effectively removing the proton-accepting capability at this position. Previous measurements of tyrosyl radical formation in reaction centers were performed using both optical and electron paramagnetic resonance (EPR) spectroscopy at room temperature (*9*, *20*, *22*). In this work, the light-induced formation of a tyrosyl radical in these mutants at different pH values was probed by low-temperature electron paramagnetic resonance spectroscopy of samples in which the radicals were generated at room temperature and trapped by freezing.

Table 1: Mutants of *Rhodobacter sphaeroides*

name[a]	redox mutations[b]	tyrosine position[c]	proton acceptor position[c]
quadruple	quadruple		
Y_{L135}	quadruple	Tyr L135	Tyr L164, Tyr L144
Y_{L135} + YH(L164)	quadruple	Tyr L135	His L164, Tyr L144
Y_{L135} + YH(L164) + YE(L144)	quadruple	Tyr L135	His L164, Glu L144
Y_{L135} + YF(L164)	quadruple	Tyr L135	Phe L164, Tyr L144
Y_{L162} + SH(M190)	quadruple	Tyr L162	His M190
Y_{M164}	quadruple	Tyr M164	His M193, Glu M173
Y_{M193} + RH(M164)	quadruple	Tyr M193	His M164

[a] The position of the targeted tyrosine in each mutant is denoted by the subscript. For mutations, the first letter designates the wild-type residue, the second letter designates the amino acid residue substitution, and the residue position is in parentheses. The Y_{L135} and Y_{M164} mutants have been referred to in previous publications as the Y_L and Y_M mutants, respectively (*9*, *20*−*22*). [b] The quadruple mutant contains the changes LH(L131) + LH(M160) + FH(M197) + YW(M210), which together result in an increase of over 0.3 V in the P/P^+ midpoint potential. The other mutants also all contain these four changes. [c] Tyrosines and proton acceptors have either been introduced by mutagenesis or are present in the native reaction center sequence.

MATERIALS AND METHODS

Construction of Mutants and Protein Isolation. The quadruple, Y_M, and Y_L mutants (Table 1) have been described previously (*9*). Here the Y_M and Y_L mutants will be referred to as the Y_{M164} and Y_{L135} mutants, respectively, to distinguish them from mutants with tyrosyl radicals at other positions. The mutants Y_{L162} + SH(M190) and Y_{M193} + RH(M164) contain the four mutations in the quadruple mutant and the additional mutations Ser to His at M190 in the Y_{L162} + SH(M190) mutant and His to Tyr at M193 plus Arg to His at M164 in the Y_{M193} + RH(M164) mutant. The mutants Y_{L135} + YH(L164), Y_{L135} + YH(L164) + YE(L144), and Y_{L135} + YF(L164) contain the five substitutions in the Y_{L135} mutant plus the additional alterations Tyr to His at L164, Tyr to His at L164 and Tyr to Glu at L144, and Tyr to Phe at L164, respectively. Construction of these mutants was achieved by oligonucleotide-directed mutagenesis and by genetic manipulation of restriction fragments (*7*). Wild-type reaction centers were those isolated from the strain ΔLM1.1 containing a plasmid carrying the genes for the wild-type L and M subunits (*23*). Cell growth and reaction center isolation were as described earlier (*23*) except that 0.05% Triton X-100 was used as the detergent in the DEAE chromatography. Samples were concentrated, and the pH was changed by using 0.05% Triton X-100 and 15 mM Tris-HCl with the pH adjusted with either 1 M NaOH or 1 M HCl.

Preparation of Trapped Radicals. Reaction center samples were concentrated to 185 μM using a Centricon microconcentrator (Amicon). Illumination was achieved through a 1 cm diameter fiber optic coupled to an Oriel tungsten lamp

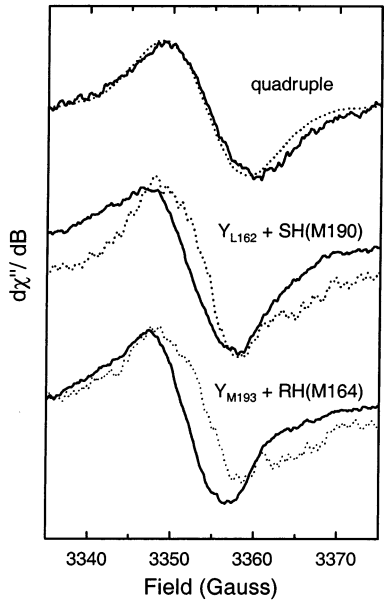

FIGURE 2: Normalized light-induced EPR spectra of reaction center samples from the quadruple, Y_{L162} + SH(M190), and Y_{M193} + RH(M164) mutants at pH 6.3 (dotted line) and pH 11.0 (solid line). Samples were illuminated at room temperature, the radical was trapped at 200 K, and the spectra were measured at 125 K.

with a 10 cm water filter (*9*, *20*). The samples were illuminated at low light levels for 24 s at room temperature. Following the illumination, the samples were immediately plunged into an ethanol/dry ice bath (200 K) in the dark. The samples were stored in liquid nitrogen.

EPR Spectroscopy. EPR measurements were performed in a Bruker E580 X-band spectrometer. EPR spectra were recorded at 125 K; the temperature was regulated with a flow of cold nitrogen gas. Spectral conditions were as follows: a microwave frequency of 9.4008, a field modulation of 100 kHz, an amplitude of 0.4 mT, a microwave power of 10 mW, a modulation amplitude of 4 G, and 50 scans per spectrum.

RESULTS

EPR Spectra of Trapped Radicals. Derivative-shaped signals were observed in light-minus-dark EPR spectra of reaction center samples from wild type and all of the mutants (Figures 2 and 3). These light-induced signals of frozen samples were similar to spectra of the Y_{M164} and Y_{L135} mutants previously taken at room temperature (*9*, *20*). The trapped signals were stable for many months. The widths of the signals ranged from 9 to 11 G. The *g* values, measured with an estimated error of ±0.0001, were between 2.0024 and 2.0051 (Table 2). At pH 6.3 all of the mutants exhibited signals predominately characteristic of the P^+ radical. The *g* value of the spectra from the quadruple mutant did not change with pH, while the *g* values measured for the other mutants became higher with increasing pH.

Identification of Radicals. Three species in the wild-type bacterial reaction center could give EPR signals with *g* values between 2.0020 and 2.0050, P^+, the reduced quinones, and the reduced bacteriopheophytin (H_A^-). The quinones are coupled to a non-heme iron that broadens the signal; moreover, this signal can only be observed at temperatures below 10 K. In studies on the wild type, an EPR signal from

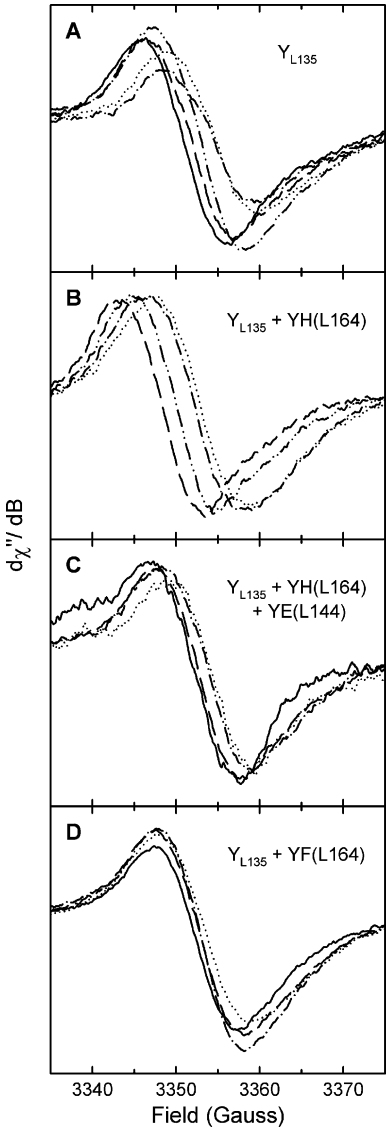

FIGURE 3: Light-induced EPR spectra of reaction center samples from theY_{L135} (A), Y_{L135} + YH(L164) (B), Y_{L135} + YH(L164) + YE(L144) (C), and Y_{L135} + YF(L164) (D) mutants at pH 6.3 (dotted line), pH 8.0 (dash dot line), pH 9.0 (dash dot dot line), pH 10.2 (dashed line), and pH 11.0 (solid line). Samples were illuminated at room temperature, the radical was trapped at 200 K, and the spectra were measured at 125 K.

H_A^-, which normally rapidly transfers an electron to the primary quinone acceptor, is only observed when the quinone acceptor is reduced with dithionite before illumination (*24*). Other conditions used for generating a stable H_A^- state include the presence of cytochrome as a secondary donor, continuous saturating illumination at room temperature, and trapping at low temperature. In the experiments reported here, the nonsaturating illumination conditions with no dithionite present minimize the probability of forming the H_A^- state. EPR spectra attributed to tyrosyl radicals have been observed in these types of reaction center mutants in other studies (*9*, *20*). Thus, for these conditions, we assume that the only species giving rise to an EPR signal in this region are P^+ and $Y^\bullet$. The *g* value of the P^+ radical is centered at 2.0025 ± 0.0001 and is independent of the pH (*25*). Reported *g* values for tyrosyl radicals in other systems are between 2.0040 and 2.0050, with the amplitude of the signal highly dependent on pH due to the presence of a proton acceptor

Table 2: Summary of *g* Values for the Mutants at Various pH Values

strain	*g* value				
	pH 6.3	pH 8.0	pH 9.0	pH 10.2	pH 11.0
quadruple	2.0026	2.0026	2.0025	2.0025	2.0024
Y_{L135}	2.0024	2.0025	2.0035	2.0040	2.0043
Y_{L135} + YH(L164)	2.0025	2.0030	2.0043	2.0051	
		2.0030			
		2.0031			
Y_{L135} + YH(L164)	2.0028	2.0030		2.0033	2.0038
+ YE(L144)		2.0030		2.0038	2.0040
		2.0034			
Y_{L135} + YF(L164)	2.0029		2.0036	2.0036	2.0037
	2.0032		2.0038	2.0039	2.0043
Y_{L162} + SH(M190)	2.0028				2.0041
Y_{M164}				2.0043	
Y_{M193} + RH(M164)	2.0029				2.0041

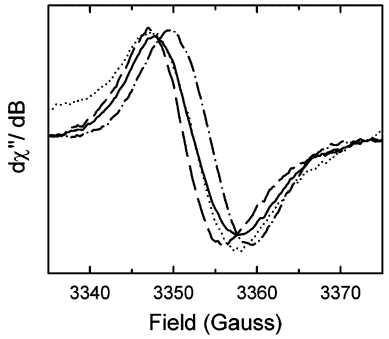

FIGURE 4: Comparison of the spectrum of theY_{L135} + YH(L164) + YE(L144) at pH 10.2 (dotted line) and the simulated spectrum (solid line) obtained by a linear combination of the spectrum of wild type at pH 8.0 (dash dot line) and the spectrum of the Y_{M164} mutant at pH 10.2 (dashed line). The fit yields a fraction of $Y^{\bullet}$ of 0.63 ± 0.02 and the same *g* value of 2.0038 as found in the measured spectrum.

(*26*). The difference in the *g* values between P^+ and $Y^{\bullet}$ constitutes a downshift in the field of approximately 4 G.

Determination of Radical Populations. If only P^+ and $Y^{\bullet}$ give rise to an EPR signal at this temperature, then the signals centered at *g* values of 2.0024−2.0026 can be assigned to the P^+ radical, while signals centered at 2.0040−2.0050 should be comprised of $Y^{\bullet}$. Signals with *g* values between 2.0025 and 2.0040 will contain a mixture of both radicals. Representative spectra of these two radicals can be used to determine the concentrations of each species at any *g* value between the *g* values of these two species. For this purpose, a spectrum of wild-type reaction centers, with a *g* value of 2.0025, was taken as a representative signal for the P^+ species. The signal for the pure Y species in the reaction center is more difficult to determine. A Y_{M164} spectrum at pH 10.2 with a *g* value of 2.0043 was used as a representative signal, although its spectrum may not be comprised of pure tyrosyl signal (*9*). To avoid additional introduction of error due to baseline drifts or poor signal to noise ratio, truncation of the spectra to the region of the single derivative signal was employed. The spectra of the mutants with intermediate *g* values were fit as a linear combination of the representative P^+ and $Y^{\bullet}$ spectra (Figure 4).

DISCUSSION

The factors required for tyrosyl radical formation in reaction centers were explored in a series of mutants of *R. sphaeroides*. In this series of mutants, the position of the tyrosine and the identity of residues that may act as proton acceptors were varied. Previous evidence for tyrosyl formation in reaction center mutants included a correlation between room temperature EPR spectra that showed an increase in the *g* value from that associated with P^+ in the wild type and optical spectra that showed distinct new features (*9*, *20*, *22*). Due to the low quantum yield of the charge-separated states in mutants with high P/P^+ midpoint potentials, the light-induced changes in both the optical and EPR spectra are limited. EPR measurements at low temperature, which are intrinsically more sensitive than at room temperature, were performed on the mutants reported here. Trapping of the radicals in these samples also allowed calculation of the relative populations of the radicals present. While a high-potential oxidant is clearly necessary for tyrosyl radical formation, it is apparently not sufficient. The results point to a limited sphere of locations favorable for tyrosine oxidation and an important role for the proton acceptor.

The EPR spectra of reaction centers from the quadruple mutant show the presence of the oxidized bacteriochlorophyll dimer, and these spectra do not change with pH. These results are consistent with previous studies using optical spectroscopy that reported no evidence of a tyrosyl radical in this mutant but rather signals comparable to the wild-type reaction center (*9*). Although the bacteriochorophyll dimer in this mutant has a high midpoint potential, apparently none of the tyrosine residues in the vicinity become oxidized. The evidence for tyrosine oxidation in the other mutants can thus be attributed to the effect of one or two amino acid residues that differ from the quadruple mutant.

Upon examination of the structure of the bacterial reaction center, several tyrosine residues are found less than 15 Å away from the edge of the bacteriochlorophyll dimer (Table 3) (*27*). Of these, Tyr M210 and Tyr L162 are the closest, at less than 7 Å away, whereas the next closest tyrosine residues are found at least 10 Å away from the bacteriochlorophyll dimer. In all of these mutants Tyr M210 has been changed to Trp, precluding examination of its oxidation. The lack of tyrosine oxidation in the quadruple mutant indicates that Tyr L162 is not redox active. To test whether a proton acceptor is necessary to "activate" this tyrosine residue, a histidine residue, intended to provide a proton acceptor, was inserted nearby at M190 in the Y_{L162} + SH(M190) mutant. The results indicate that this mutant produces a tyrosyl spectrum at pH 11.0, demonstrating the role of the proton acceptor as key in tyrosine oxidation. A similar Tyr−His pair at residues M193 and M164, respectively, is found in the Y_{M193} + RH(M164) mutant, which also showed the capability of producing a tyrosyl signal at pH 11.0. The different environment compared to the Y_{M164} mutant, with Tyr at M164 and His at M193, does not appear to hinder formation of the tyrosyl radical. Even in the absence of a clear pathway for the proton, tyrosyl radical formation was observed when a tyrosine residue was introduced at L167, which is located 5 Å from the dimer, in the Y_{L167} mutant (*22*).

To generate a neutral tyrosyl radical, both electron and proton transfer from the tyrosine must occur, since generation of the tyrosyl cation radical or the anion radical is energetically unfavorable (*28*, *29*). Previous studies have suggested

Table 3: Location of Native and Introduced Tyrosine Residues in the Vicinity of the Bacteriochlorophyll Dimer in the Reaction Center from *R. sphaeroides*

location	proton acceptor	distance (Å)[a]	tyrosyl radical formation
M210		4.5	not tested[b]
L167		4.5	in Y_{L167} mutant (*22*)
L162	His M190	6.5	in Y_{L162} + SH(M190) mutant
L135	Tyr L164	9.4	in Y_{L135} mutants[c]
M164	His M193, Glu M173	10.0	in Y_{M164} mutants[d]
M193	His M164	10.6	in Y_{M193} + RH(M164) mutant
L164		10.7	
L169	Glu M111	12.4	
L148	Tyr L128	14.0	
L128	Tyr L148	14.2	
M198	Asp L155	14.2	
L67		14.9	
L144		16.0	
M295		17.1	

[a] Distances calculated from the edge of the bacteriochlorophyll dimer to the phenolic oxygen of M210, L162, L164, L169, L148, L128, M198, L67, L144, and M295, the δ-carbon atom of the benzene ring of the native Phe L167, the ϵ-amine group of the native Arg L135 and Arg M164, and the ring of the native His M193, using the structure of McAuley et al. (*27*). [b] The residue Tyr M210 was changed to Trp in all of the mutants studied. [c] Also observed in the Y_{L135} + YH(L164), Y_{L135} + YH(L164) + YE(L144), and Y_{L135} + YF(L164) mutants. [d] Also observed in mutants with alterations at M193 and M173, the putative proton acceptor positions (*20*).

that when P^+ is reduced by electron transfer from the tyrosine, a nearby residue acts as a proton acceptor to the phenolic proton (*9*, *20*, *21*). In this model, the formation of a tyrosyl radical is highly dependent on the capability of donating the proton to a nearby residue. At pH values much lower than the pK_a of the putative proton acceptor, the tyrosyl radical will not be generated, leaving P^+ and its characteristic signal located at a *g* value of 2.0025 ± 0.0001. At pH values above its pK_a, the proton acceptor can accept the phenolic proton upon tyrosyl formation. The tyrosyl is then able to reduce P^+ forming P, an EPR-silent species. This results in the neutral tyrosyl radical and a shift in the EPR spectra to *g* values between 2.0040 and 2.0050. Alternatively, the tyrosine itself can become deprotonated at high pH prior to electron transfer.

The EPR spectra showed a distinctive pH dependence in all of the mutants containing tyrosyl radicals (Table 2). The pH dependence was investigated more fully in the mutants with Tyr at L135, and the changes resulting from the replacement of residues with different biochemical properties indicate that the protein environment plays a key role in the formation of the tyrosyl radical. The extent of the tyrosyl signal formed in the Y_{L135} mutant can be fitted to a Henderson−Hasselbalch equation with an observed pK_a of approximately 8.9 (Figure 5A). The most likely proton acceptor for Tyr L135 in the Y_{L135} mutant is Tyr L164. The pK_a of 8.9 in the Y_{L135} mutant is similar to the pK_a of 8.3 obtained from optical measurements of tyrosyl formation in this mutant (*9*). Changing this putative proton acceptor to His in the Y_{L135} + YH(L164) mutant resulted in a pK_a of approximately 8.5 (Figure 5B). The shift to a slightly lower pK_a in this mutant is consistent with the inherently lower pK_a of histidine compared to tyrosine. An increase in the pK_a for tyrosyl formation was also observed upon replacement of the proton acceptor His M193 with Tyr in theY_{M164}

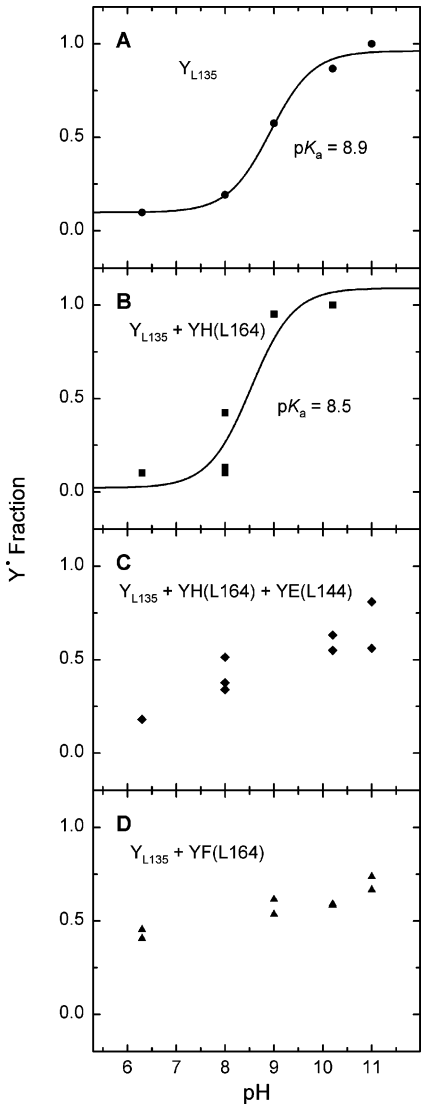

FIGURE 5: Extent of formation of the tyrosyl radical as a function of pH for the Y_{L135} (A), Y_{L135} + YH(L164) (B), Y_{L135} + YH(L164) + YE(L144) (C), and Y_{L135} + YF(L164) (D) mutants. The lines are fits to a Henderson−Hasselbalch equation.

mutant, although the pK_a value of the Y_{L135} + YH(L164) is higher than the pK_a of approximately 7 observed in the Y_{M164} mutant (*9*, *20*).

More extensive alterations in the pH dependence of tyrosyl radical formation at L135 were observed after the addition of Glu nearby in the Y_{L135} + YH(L164) + YE(L144) mutant, which may modify the interaction of Tyr L135 with His L164, and after changing Tyr L164 for Phe in the Y_{L135} + YF(L164) mutant, which should result in the loss of the ability of the L164 site to act as a proton acceptor (Figure 5C,D). The extent of tyrosyl formation in these mutants appears to be limited, even at the higher pH values. This effect is reminiscent of the observation that removal of the putative major proton acceptor for the Y_{M164} mutant results in a decrease in the extent of tyrosyl formation (*20*). It is also possible that the tyrosyl radical decays rapidly in these mutants, so that it cannot be trapped. The measurable formation of the tyrosyl signal at lower pH values is also different than what was observed for the Y_{L135} mutant. Although a pK_a value was not obtained for the pH dependence in these mutants, the clear alteration in the behavior

resulting from mutations in nearby residues demonstrates the influence of the environment on tyrosyl radical formation.

In conclusion, evidence for partial or nearly complete tyrosyl radical formation has now been found for tyrosine residues located at five positions in the reaction center: L135, L162, L167, M164, and M193 (Table 3). The role of the proton acceptor in the formation of the radical is demonstrated by the pH dependence of the mutants. Differences in the L and M sides also point to the role of the protein environment in stabilizing the tyrosyl radical. Overall, these results demonstrate that the location of a tyrosyl radical in the reaction centers is not uniquely constrained to the positions analogous to those in the photosystem II but that a combination of distance and protein environment enables radical formation at several locations.

ACKNOWLEDGMENT

We thank Laszlo Kálmán for helpful discussions.

REFERENCES

1. Blankenship, R. E., Madigan, M. T., and Bauer, C. E., Eds. (1995) *Anoxygenic Photosynthetic Bacteria*, Kluwer Academic Publishers, Dordrecht, The Netherlands.
2. Feher, G., Allen, J. P., Okamura, M. Y., and Rees, D. C. (1989) Structure and function of bacterial reaction centres, *Nature 339*, 111−116.
3. Watanabe, T., and Kobayashi, M. (1991) Electrochemistry of Chlorophylls, in *Chlorophylls* (Scheer, H., Ed.) pp 287−316, CRC Press, Boca Raton, FL.
4. Boussac, A., and Etienne, A. L. (1984) Midpoint potential of signal II (slow) in Tris-washed photosystem-II particles, *Biochim. Biophys. Acta 766*, 576−581.
5. Vass, I., and Styring, S. (1991) pH-dependent charge equilibria between tyrosine-D and the S states in photosystem II. Estimation of relative midpoint redox potentials, *Biochemistry 30*, 830−839.
6. Nagarajan, V., Parson, W. W., Davis, D., and Schenck, C. C. (1993) Kinetics and free energy gaps of electron-transfer reactions in *Rhodobacter sphaeroides* reaction centers, *Biochemistry 32*, 12324−12336.
7. Lin, X., Murchison, H. A., Nagarajan, V., Parson, W. W., Allen, J. P., and Williams, J. C. (1994) Specific alteration of the oxidation potential of the electron donor in reaction centers from *Rhodobacter sphaeroides*, *Proc. Natl. Acad. Sci. U.S.A. 91*, 10265−10269.
8. Allen, J. P., and Williams, J. C. (1995) Relationship between the oxidation potential of the bacteriochlorophyll dimer and electron transfer in photosynthetic reaction centers, *J. Bioenerg. Biomembr. 27*, 275−283.
9. Kálmán, L., LoBrutto, R., Allen, J. P., and Williams, J. C. (1999) Modified reaction centres oxidize tyrosine in reactions that mirror photosystem II, *Nature 402*, 696−699.
10. Debus, R. J., Barry, B. A., Babcock, G. T., and McIntosh, L. (1988) Site-directed mutagenesis identifies a tyrosine radical involved in the photosynthetic oxygen-evolving system, *Proc. Natl. Acad. Sci. U.S.A. 85*, 427−430.
11. Vermaas, W. F. J., Rutherford, A. W., and Hansson, Ö. (1988) Site-directed mutagenesis in photosystem II of the cyanobacterium *Synechocystis* sp. PCC 6803: Donor D is a tyrosine residue in the D2 protein, *Proc. Natl. Acad. Sci. U.S.A. 85*, 8477−8481.
12. Metz, J. G., Nixon, P. J., Rögner, M., Brudvig, G. W., and Diner, B. A. (1989) Directed alteration of the D1 polypeptide of photosystem II: evidence that tyrosine-161 is the redox component, Z, connecting the oxygen-evolving complex to the primary electron donor, P680, *Biochemistry 28*, 6960−6969.
13. Gilchrist, M. L., Ball, J. A., Randall, D. W., and Britt, R. D. (1995) Proximity of the manganese cluster of photosystem II to the redox-active tyrosine Y_Z, *Proc. Natl. Acad. Sci. U.S.A. 92*, 9545−9549.
14. Tommos, C., Tang, X. S., Warncke, K., Hoganson, C. W., Styring, S., McCracken, J., Diner, B. A., and Babcock, G. T. (1995) Spin-density distribution, conformation, and hydrogen bonding of the redox-active tyrosine Y_Z in photosystem II from multiple-electron magnetic-resonance spectroscopies: Implications for photosynthetic oxygen evolution, *J. Am. Chem. Soc. 117*, 10325−10335.
15. Tang, X. S., Randall, D. W., Force, D. A., Diner, B. A., and Britt, R. D. (1996) Manganese-tyrosine interaction in the photosystem II oxygen-evolving complex, *J. Am. Chem. Soc. 118*, 7638−7639.
16. Hoganson, C. W., and Babcock, G. T. (1997) A metalloradical mechanism for the generation of oxygen from water in photosynthesis, *Science 277*, 1953−1956.
17. Mamedov, F., Sayre, R. T., and Styring, S. (1998) Involvement of histidine 190 on the D1 protein in electron/proton-transfer reactions on the donor side of photosystem II, *Biochemistry 37*, 14245−14256.
18. Debus, R. J. (2001) Amino acid residues that modulate the properties of tyrosine Y_Z and the manganese cluster in the water oxidizing complex of photosystem II, *Biochim. Biophys. Acta 1503*, 164−186.
19. Diner, B. A. (2001) Amino acid residues involved in the coordination and assembly of the manganese cluster of photosystem II. Proton-coupled electron transport of the redox-active tyrosines and its relationship to water oxidation, *Biochim. Biophys. Acta 1503*, 147−163.
20. Narváez, A. J., Kálmán, L., LoBrutto, R., Allen, J. P., and Williams, J. C. (2002) Influence of the protein environment on the properties of a tyrosyl radical in reaction centers from *Rhodobacter sphaeroides*, *Biochemistry 41*, 15253−15258.
21. Kálmán, L., Williams, J. C., and Allen, J. P. (2003) Proton release upon oxidation of tyrosine in reaction centers from *Rhodobacter sphaeroides*, *FEBS Lett. 545*, 193−198.
22. Kálmán, L., LoBrutto, R., Narváez, A. J., Williams, J. C., and Allen, J. P. (2003) Correlation of proton release and electrochromic shifts of the optical spectrum due to oxidation of tyrosine in reaction centers from *Rhodobacter sphaeroides*, *Biochemistry 42*, 13280−13286.
23. Williams, J. C., Alden, R. G., Murchison, H. A., Peloquin, J. M., Woodbury, N. W., and Allen, J. P. (1992) Effects of mutations near the bacteriochlorophylls in reaction centers from *Rhodobacter sphaeroides*, *Biochemistry 31*, 11029−11037.
24. Okamura, M. Y., Isaacson, R. A., and Feher, G. (1979) Spectroscopic and kinetic properties of the transient intermediate acceptor in reaction centers of *Rhodopseudomonas sphaeroides*, *Biochim. Biophys. Acta 546*, 394−417.
25. Lubitz, W. (1991) EPR and ENDOR Studies of Chlorophyll Cation and Anion Radicals, in *Chlorophylls* (Scheer, H., Ed.) pp 904−944, CRC Press, Boca Raton, FL.
26. Stubbe, J., and van der Donk, W. A. (1998) Protein radicals in enzyme catalysis, *Chem. Rev. 98*, 705−762.
27. McAuley, K. E., Fyfe, P. K., Ridge, J. P., Isaacs, N. W., Cogdell, R. J., and Jones, M. R. (1999) Structural details of an interaction between cardiolipin and an integral membrane protein, *Proc. Natl. Acad. Sci. U.S.A. 96*, 14706−14711.
28. Ahlbrink, R., Haumann, M., Cherepanov, D., Bögershausen, O., Mulkidjanian, A., and Junge, W. (1998) Function of tyrosine Z in water oxidation by photosystem II: electrostatical promotor instead of hydrogen abstractor, *Biochemistry 37*, 1131−1142.
29. Tommos, C., and Babcock, G. T. (2000) Proton and hydrogen currents in photosynthetic water oxidation, *Biochim. Biophys. Acta 1458*, 199−219.

BI048691P